The composition and weathering of the continents over geologic time
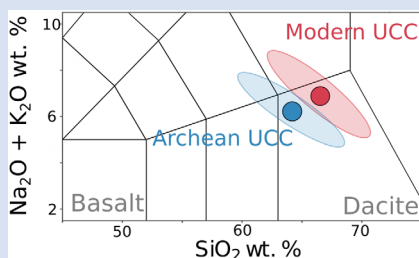
A.G. Lipp[1*], O. Shorttle[2,3], E.A. Sperling[4], J.J. Brocks[5], D.B. Cole[6], P.W. Crockford[7], L. Del Mouro[8], K. Dewing[9], S.Q. Dornbos[10], J.F. Emmings[11], U.C. Farrell[12], A. Jarrett[13], B.W. Johnson[14], P. Kabanov[9], C.B. Keller[15], M. Kunzmann[16], A.J. Miller[17], N.T. Mills[18], B. O'Connell[19], S.E. Peters[20], N.J. Planavsky[21], S.R. Ritzer[4], S.D. Schoepfer[22], P.R. Wilby[11], J. Yang[23]

OPEN ACCESS

Abstract

The composition of continental crust records the balance between construction by tectonics and destruction by physical and chemical erosion. Quantitative constraints on how igneous addition and chemical weathering have modified the continents' bulk composition are essential for understanding the evolution of geodynamics and climate. Using novel data analytic techniques we have extracted temporal trends in sediments' protolith composition and weathering intensity from the largest available compilation of sedimentary major element compositions: ~15,000 samples from 4.0 Ga to the present. We find that the average Archean upper continental crust was silica-rich and had a similar compositional diversity to modern continents. This is consistent with an early Archean, or earlier, onset of plate tectonics. In the Archean, chemical weathering sequestered ~25 % more CO_2 per mass eroded for the same weathering intensity than in subsequent time periods, consistent with carbon mass balance despite higher Archean outgassing rates and more limited continental exposure. Since 2.0 Ga, over long (>0.5 Gyr) timescales, crustal weathering intensity has remained relatively constant. On shorter timescales over the Phanerozoic, weathering intensity is correlated to global climate state, consistent with a weathering feedback acting in response to changes in CO_2 sources or sinks.

Introduction

The rocks at Earth's surface are compositionally divided between dense, silica-poor oceanic crust and a buoyant, silica-rich continental crust. It is generally accepted that this dichotomy is maintained by plate tectonics. The emergence of Earth's first felsic continents therefore could be an indicator for when plate tectonics began. The timing of the earliest felsic continents however remains debated. The Archean (*i.e.* 2.5–4.0 Ga) continents are often viewed as having a mafic composition similar to the

oceanic crust (*e.g.*, Taylor and McLennan, 1986; Tang *et al.*, 2016) suggesting a late onset for plate tectonics during the Neoarchean, ~2.5 Ga. However, a contrasting view has emerged of evolved, silica-rich Archean continents (Greber *et al.*, 2017; Keller and Harrison, 2020; Ptáček *et al.*, 2020). This view suggests an earlier onset for plate tectonics before 3.5 Ga.

Not only is the history of the crust necessary for understanding geodynamics, reactions between the crust and hydrosphere stabilise the planet's climate (Broecker and Langmuir, 1985). Continental chemical weathering (the alteration of silicate

1. Department of Earth Sciences and Engineering, Imperial College London, UK
2. Department of Earth Sciences, University of Cambridge, UK
3. Institute of Astronomy, University of Cambridge, UK
4. Department of Geological Sciences, Stanford University, USA
5. Research School of Earth Sciences, Australian National University, Canberra, Australia
6. School of Earth and Atmospheric Science, Georgia Institute of Technology, USA
7. Earth and Planetary Science, Weizmann Institute of Science, Israel
8. Geology Department, Federal University of Santa Catarina, Brazil
9. Natural Resources Canada, Geological Survey of Canada, Calgary, Canada
10. Department of Geosciences, University of Wisconsin-Milwaukee, USA
11. British Geological Survey, Keyworth, UK
* Corresponding author (email: a.lipp18@imperial.ac.uk)

12. Department of Geology, Trinity College Dublin, Republic of Ireland
13. Onshore Energy Directorate, Geoscience Australia, Australia
14. Department of Geological and Atmospheric Sciences, Iowa State University, USA
15. Department of Earth Sciences, Dartmouth College, USA
16. Mineral Resources, CSIRO, Australia
17. Department of Earth and Environmental Sciences, University of Waterloo, Canada
18. Department of Geology and Geophysics, Texas A&M University, USA
19. School of Earth Sciences, University of Melbourne, Australia
20. Department of Geoscience, University of Wisconsin-Madison, USA
21. Department of Earth and Planetary Sciences, Yale University, USA
22. Geoscience and Natural Resources, Western Carolina University, USA
23. China University of Geosciences, Wuhan, China

minerals by reaction with water at Earth's surface) transfers atmospheric CO_2 into carbonate minerals deposited on the ocean floor. This reaction is the major long term sink for CO_2 outgassed by the mantle (Walker *et al.,* 1981; Berner *et al.,* 1983).

The geochemical composition of sedimentary rocks is our primary record of crustal evolution on Gyr timescales. However, this archive is challenging to interpret. Chemical weathering strips sediments of mobile elements altering their composition relative to the rocks from which they derive (protoliths). Signals of changing crustal composition are thus obscured by alteration. Additionally, most sediments record the signals of the local catchment they come from, not the continental crust as a whole. Here, we provide new perspectives into the long term composition and alteration of the upper continental crust (UCC). We use novel data analytic methods and the geochemical database produced by the Sedimentary Geochemistry and Paleoenvironments Project.

Methods and Data

Most studies aiming to track changes in crustal composition avoid the alteration of sedimentary compositions by selecting weathering-insensitive elemental ratios. Whilst this approach can resolve protolith changes, by design, it cannot provide information on weathering intensity changes. Here, we simultaneously extract signals of both the weathering intensity of sediments and protolith composition.

To do this we use a new method which explains the major element (Si, Al, Fe, Mg, Na, Ca, K) composition of sediments in terms of the composition of their protolith, and how intensely they have been weathered (Lipp *et al.,* 2020). This approach constructs a model for a centred log-ratio transformed composition (after Aitchison, 1986) $\mathbf{x}'$, as the sum of a weathering vector, $\hat{\mathbf{w}}$, and a protolith vector, $\hat{\mathbf{p}}$, relative to the composition of modern UCC:

$$\mathbf{x}' = \mathbf{UCC} + \omega\hat{\mathbf{w}} + \psi\hat{\mathbf{p}} + \mathbf{E}. \qquad \text{Eq. 1}$$

The coefficients of these vectors correspond to the weathering intensity experienced by a sediment, ω, and its protolith composition, ψ. Deviations from this model cause the misfit, $\mathbf{E}$, to rise. Sediments with protoliths more(/less) felsic than modern UCC have positive(/negative) ψ values. Weathering of rocks causes ω to rise. Here, we modify this method to correct for the effect of sodium-calcium cation exchange that can occur between dissolved species and those adsorbed to clays (*e.g.,* Sayles and Mangelsdorf, 1979). We also use a recalibrated $\hat{\mathbf{w}}$ vector. These modifications reduce the possibility of biases. Some limitations, including diagenesis and marine authigenic clay formation, are discussed in the Supplementary Information but do not significantly affect our results.

We apply this method to the compilation of sedimentary geochemical data produced by the Sedimentary Geochemistry and Paleoenvironments (SGP) research consortium

(sgp.stanford.edu). The SGP database compiles geochemical data and geological context information from three sources: 1) direct data entry by SGP team members (mainly Neoproterozoic and Palaeozoic shales with global geographic coverage), 2) the USGS National Geochemical Database (consisting of data from USGS projects from the 1960-1990s; mainly Phanerozoic samples of all lithologies from the United States), and 3) the USGS Critical Metals in Black Shales database (a global shale database spanning all of Earth history). In total we analyse 17,472 major element compositions each associated with an age. Full details of data, pre-processing and analysis is found in the Supplementary Information.

The Archean Protolith

First, we investigate changes in the average composition of the exposed UCC through time. To overcome local heterogeneities we calculate composite samples using the arithmetic mean of all samples in 500 Myr time intervals (Table S-1). Because of low sampling density in the Archean, we average all samples older than 2.5 Ga to create an Archean composite. We solve Equation 1 for each composite to calculate ω and ψ, the weathering and protolith coefficients.

We can use Equation 1 to reconstruct the full major element composition of a sediment's protolith from just its ψ value. By substituting the ω value of a sediment in Equation 1 for that of pristine igneous rocks ($\omega_0 = -0.271$; see Supplementary Information) the composition of a sediment's protolith is returned. The calculated compositions of the average sediment protoliths through time are shown in Table 1. These protoliths can be analysed as igneous rocks, with *e.g.,* a Total Alkali-Silica plot (Fig. 1). The average Archean protolith was silica-rich and dacitic in composition but slightly more mafic than younger protoliths. This evolved composition for Archean protoliths is similar, albeit marginally more felsic, to the estimate of Ptáček *et al.* (2020) but arrived at using independent methodologies. The average protolith has remained constant since 2.5 Ga.

As sediments derive from broad regions, their protoliths, in aggregate, can be assumed to be representative of the average exposed crustal composition. Our estimate for the average protolith of recent, <0.5 Ga, sedimentary rocks (Fig. 1) is within error of the estimate of UCC as averaged by surface sampling (Rudnick and Gao, 2003), validating this approach. A uniformitarian interpretation of the dacitic Archean UCC is that plate tectonics commenced no later than the early Archean.

Nonetheless, we note the limitations about inferring global conditions from the small inventory of Archean samples which are highly susceptible to preservation and sampling biases (Korenaga, 2013). This low sample density in the Archean gives low statistical significance to variability of age-interval means within the Archean (Fig. 2a). Evolved igneous rocks could

Table 1 Average sediment protolith composition (wt. %) through time. Uncertainties (in the form of a covariance matrix) are given in Table S-3.

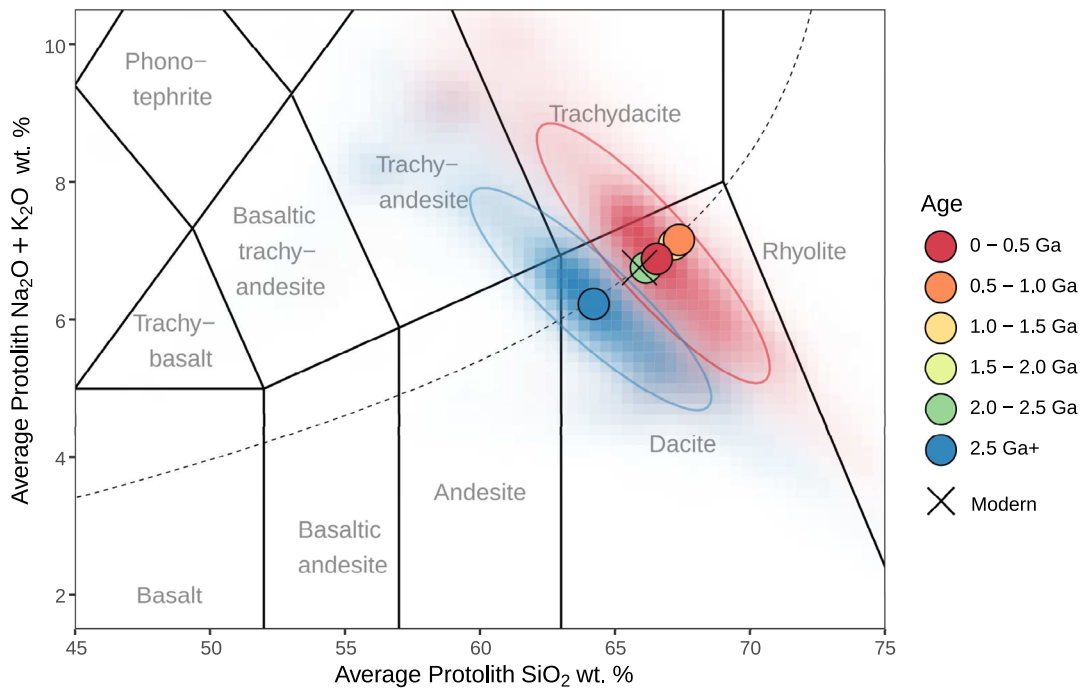| Age, Ga	SiO$_2$	Al$_2$O$_3$	Fe$_2$O$_3$^{T}	MgO	Na$_2$O	CaO	K$_2$O
0–0.5	66.5	14.6	5.32	2.32	3.98	4.32	2.95
0.5–1.0	67.3	14.5	4.99	2.05	4.04	3.98	3.17
1.0–1.5	67.1	14.5	5.06	2.11	4.03	4.05	3.11
1.5–2.0	67.3	14.5	5.00	2.06	4.04	3.99	3.16
2.0–2.5	66.1	14.7	5.48	2.46	3.95	4.48	2.85
2.5+	64.1	14.9	6.22	3.16	3.82	5.27	2.46

Figure 1 A dacitic composition for Archean UCC. Total Alkali-Silica plot displaying the protoliths of the average sediment for different time periods (Le Maitre et al., 2005). Ellipses indicate standard error (see Supplementary Information). '×' is the pristine igneous precursor of the modern upper continental crust (Rudnick and Gao, 2003). Dashed line is trend described by $\hat{\mathbf{p}}$.
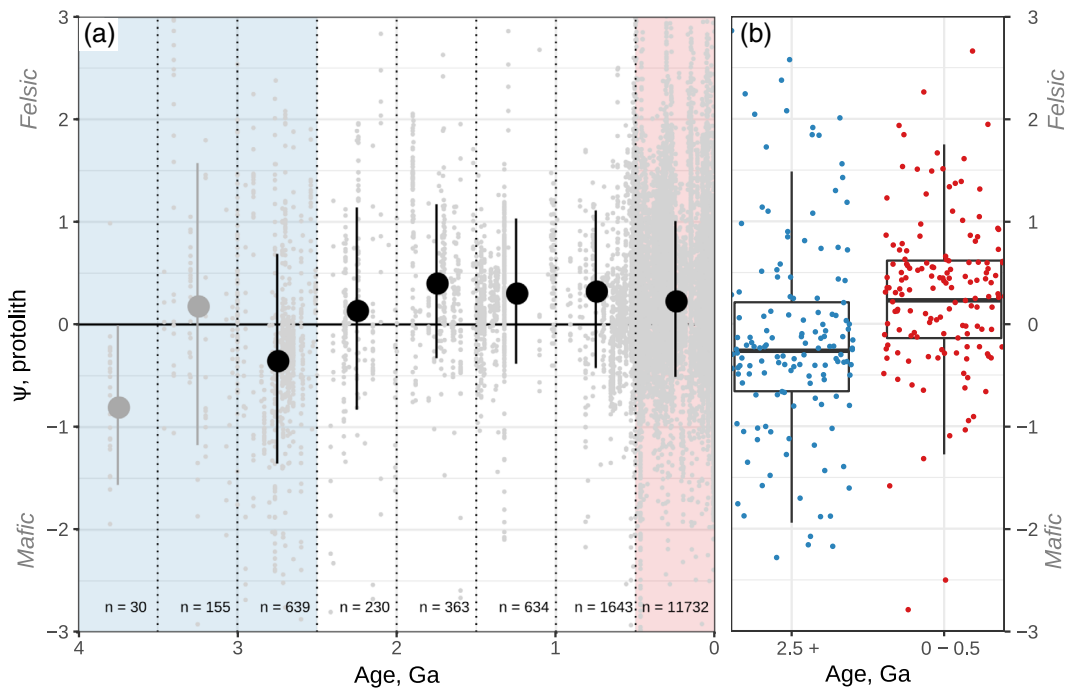

Figure 2 Archean protoliths were more mafic than the present day but equally diverse. **(a)** Grey points are protolith coefficients, ψ, for individual samples. Mean $\psi \pm \sigma$ for each 0.5 Ga time period given by black circles. Means for >3 Ga greyed out to emphasise low sample coverage. **(b)** Box and whisker comparison of protolith distributions for samples of age >2.5 and 0–0.5 Ga. Whiskers extend $1.5 \times$ interquartile-range from the upper/lower quartiles. 200 randomly selected samples shown for each age group.

also be generated in the absence of plate tectonics (Reimink et al., 2014).

Focusing exclusively on the average sediment protolith neglects other features in our dataset. The protolith coefficients, ψ, for individual samples through time (Fig. 2a) show a large

diversity in protoliths throughout Earth's history, including the Archean. If each individual ψ represents a catchment averaged protolith, then the diversity of rocks at the Earth's surface has remained nearly constant since ~4 Ga. The ψ distributions from before 2.5 Ga are compared to those from 0–0.5 Ga in Figure 2b.

Whilst the median of the two distributions is different, there is still considerable overlap. The high diversity of exposed rocks, and their on-average evolved nature, suggests that during the Archean the exposed continental crust was more similar to the modern crust than it was different. Near-constant protolith diversity from the Archean to Recent is independently evidenced by the ratio of felsic to mafic igneous rocks in a comprehensive compilation of geologic columns in North America (Fig. S-5; Peters *et al.*, 2018). This near-constant protolith diversity supports uniformitarian models of petrogenetic processes, *e.g.*, long lived plate tectonics.

Crustal Weathering on Billion Year Timescales

Second, we explore how the efficiency of CO_2 drawdown by crustal weathering may have evolved through time. The weathering of mafic rocks sequesters more CO_2 than felsic rocks due to their higher concentrations of Ca and Mg (*e.g.*, Dessert *et al.,* 2003). The more mafic Archean UCC could result in more CO_2 sequestered *per* mass of rock weathered than modern UCC. This effect could potentially bring the weathering CO_2 sink in balance with mantle outgassing despite a smaller exposed continental area (Albarede *et al.*, 2020). To quantify this effect, we calculate the chemical depletion fraction for any ω–ψ pair, assuming that Al_2O_3 is immobile (see Supplementary Information). The mass of each element mobilised due to weathering *per* kg of protolith eroded can then be converted into moles of carbonate-bound CO_2 assuming the stoichiometry

$$CaSiO_3 + CO_2 \rightarrow CaCO_3 + SiO_2,$$
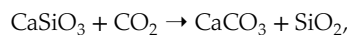
and efficient Mg-Ca exchange at mid-ocean ridges (Holland, 1984). Any ω–ψ pair can thus be converted into a (maximum) amount of CO_2 deposited *per* kg of weathered protolith (Fig. S-3a).

Weathering the Archean protolith sequesters ~25 % more CO_2 than subsequent protoliths for the same weathering

intensity (Fig. S-3b). Since the Archean, the CO_2 sequestered *per* kg UCC eroded has not changed considerably (Fig. S-3a). On timescales greater than 0.5 Gyr therefore, any change in Earth's total weathering flux must have been achieved by changing the absolute amount of erosion, not the weathering intensity. Hence, to maintain an equitable climate over these timescales, secular changes in volcanic CO_2 outgassing must have been compensated for by changes in amounts of physical erosion. Alternatively, changes to other aspects of the carbon cycle could have taken place (*e.g.*, changing the reverse weathering flux; Isson and Planavsky, 2018).

Crustal Weathering over the Phanerozoic

Finally, we explore how global weathering intensity has changed during the Phanerozoic. On 10–100 Myr timescales, weathering intensity is believed to respond to global climate state as part of a negative feedback (Walker *et al.,* 1981; Berner *et al.,* 1983). Individual sediments only record the weathering intensity of their source regions, but collectively they may reflect these global shifts in silicate weathering intensity.

Figure 3 shows the weathering coefficient, ω, for the ~12,000 samples less than 600 Ma. The lowest weathering intensity occurs in the Neogene. Other periods of low intensity are observed in the late Ordovician/Silurian, late Permian and the Jurassic. Peaks in weathering intensity are found in the Carboniferous, Triassic and Cretaceous. We find that sampling biases do not strongly affect these observations (see Supplementary Information; Fig. S-4).

The ω fluctuations we observe are on timescales too long (10's Myr) to be explained by the silicate weathering feedback acting in response to short term climatic perturbations. The weathering intensity trend is instead consistent with long term CO_2 mass balance forced by changes in the magnitude of carbon sources and sinks. For example, an increased flux of volcanic CO_2
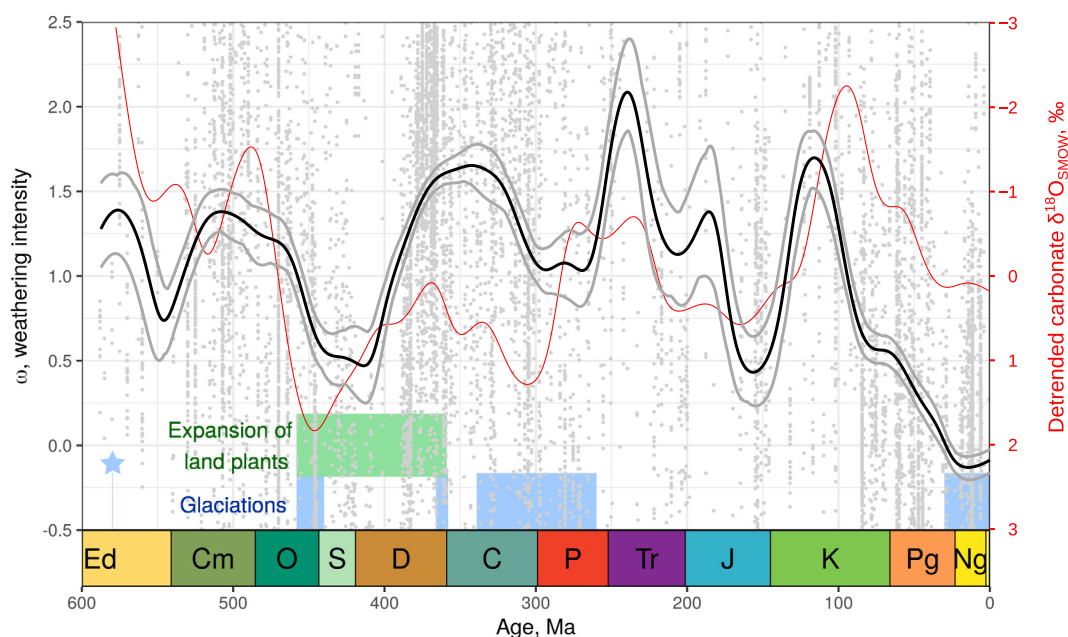

Figure 3 Weathering intensity of sedimentary rocks across the Phanerozoic. Grey points are individual samples, black line is smoothed trend calculated using 30 Myr bandwidth Gaussian kernel, and grey lines show bootstrap uncertainty (see Supplementary Information). Red line is de-trended Oxygen isotope composition of carbonates smoothed using 30 Myr bandwidth Gaussian. See Supplementary Information for origin of Phanerozoic palaeoclimate data.

would result initially in an imbalance in the geologic carbon cycle, as the weathering sink is unchanged. However, as atmospheric CO_2 rises on Myr timescales, the weathering intensity of rocks should rise due to higher pCO_2 driving warmer and wetter conditions. The carbon cycle will then achieve balance albeit at an elevated CO_2 level and altered climate state. An increase in carbon sinks driven by, *e.g.,* mountain building, would have the opposite effect. The global intensity of weathering hence changes in concert with the balance of carbon sources and sinks (*e.g.,* Raymo and Ruddiman, 1992; Berner and Caldeira, 1997; McKenzie *et al.,* 2016).

This hypothesis predicts a positive correlation between the average surface temperature and weathering intensity. We can test these predictions by comparing the smoothed weathering trend to climate proxies. First we consider the de-trended oxygen isotope composition of marine carbonates, considered a proxy for global climate (Veizer *et al.,* 2000). When the $\delta^{18}O$ of marine carbonates is heavy (associated with cooler climates) we observe a lower weathering intensity while the opposite is true for lighter $\delta^{18}O$ (associated with warmer climates).

The validity of the $\delta^{18}O$ record however is controversial as it is susceptible to diagenetic overprinting (*e.g.,* Ryb and Eiler, 2018). As a result we also compare our ω record to a less ambiguous record of climate state: evidence of glaciated poles. We observe local minima in chemical weathering intensity during ice house climates (Ordovician-Silurian, Permian, Neogene). We note however that the end Devonian glaciation coincides with a period of observed high weathering intensity. These observations generally match the relationship between weathering intensities and climate state that is predicted by carbon mass balance.

The lack of a state change in weathering intensity following the Palaeozoic emergence of land plants further illustrates the importance of carbon mass balance. The expansion of land plants, by increased pedogenesis, initially caused an increase in the weathering carbon sink. The resulting carbon cycle imbalance is then resolved by a decrease in weathering intensity by the mechanism described above (*e.g.,* Algeo *et al.,* 1995). Hence, only a transient ω response is observed in response to the stepwise expansion of land-plants.

Summary

A large inventory of sedimentary rock major element compositions has been deconvolved into a record of crustal composition and weathering intensity. Results indicate an evolved and heterogeneous Archean crust, which suggests an early onset of plate tectonics. Weathering of this Archean crust was ~25 % more efficient at sequestering atmospheric CO_2 than modern day UCC. On long, Gyr, timescales the weathering intensity of the crust has remained constant. By contrast, on short, 100 Myr, timescales weathering intensity responds to global climate shifts consistent with a silicate weathering feedback responding to changes in carbon sources or sinks.

Acknowledgements

Editor: Sophie Opfergelt

Author Contributions

AGL and OS conceived of the study. AGL performed data analysis and prepared the manuscript. EAS led development of the Sedimentary Geochemistry and Paleoenvironments Project. JJB, DC, PWC, LDM, KD, SQD, JFE, UCF, AJ, BWJ, PK, CBK, MK, AJM, NTM, BOC, SEP, NJP, SRR, SDS, PRW and JY all contributed to the Sedimentary Geochemistry and Paleoenvironments Project. JFE helped guide discussion of the role of diagenesis. NJP helped guide discussion of Phanerozoic carbon cycle. SEP produced Figure S-5. All authors contributed to manuscript revision.

Additional Information

Supplementary Information accompanies this letter at https://www.geochemicalperspectivesletters.org/article2109.

Cite this letter as: Lipp, A.G., Shorttle, O., Sperling, E.A., Brocks, J.J., Cole, D.B., Crockford, P.W., Del Mouro, L., Dewing, K., Dornbos, S.Q., Emmings, J.F., Farrell, U.C., Jarrett, A., Johnson, B.W., Kabanov, P., Keller, C.B., Kunzmann, M., Miller, A.J., Mills, N.T., O'Connell, B., Peters, S.E., Planavsky, N.J., Ritzer, S.R., Schoepfer, S.D., Wilby, P.R., Yang, J. (2021) The composition and weathering of the continents over geologic time. *Geochem. Persp. Let.* 17, 21–26.

References

AITCHISON, J. (1986) *The statistical analysis of compositional data*. Chapman and Hall, London, UK.

ALBAREDE, F., THIBON, F., BLICHERT-TOFT, J., TSIKOS, H. (2020) Chemical archeoceanography. *Chemical Geology* 548, 119625.

ALGEO, T.J., BERNER, R.A., MAYNARD, J.B., SCHECKLER, S.E. (1995) Late Devonian Oceanic Anoxic Events and Biotic Crises: "Rooted" in the Evolution of Vascular Land Plants? *GSA TODAY*, 24.

BERNER, R.A., CALDEIRA, K. (1997) The need for mass balance and feedback in the geochemical carbon cycle. *Geology* 25, 955–956.

BERNER, R.A., LASAGA, A.C., GARRELS, R.M. (1983) The carbonate-silicate geochemical cycle and its effect on atmospheric carbon dioxide over the past 100 million years. *American Journal of Science* 283, 641–683.

BROECKER, W.S., LANGMUIR, C.H. (2012) Making it comfortable. In: *How to build a habitable planet*. Princeton University Press, Princeton, NJ, 298–386.

Dessert, C., Dupré, B., Gaillardet, J., François, L.M., Allègre, C.J. (2003) Basalt weathering laws and the impact of basalt weathering on the global carbon cycle. *Chemical Geology*. 202, 257–273.

Greber, N.D., Dauphas, N., Bekker, A., Ptáček, M.P., Bindeman, I.N., Hofmann, A. (2017) Titanium isotopic evidence for felsic crust and plate tectonics 3.5 billion years ago. *Science* 357, 1271–1274.

Holland, H.D. (1984) *The Chemical Evolution of the Atmosphere and Oceans*. Princeton University Press, Princeton, NJ.

Isson, T.T., Planavsky, N.J. (2018) Reverse weathering as a long-term stabilizer of marine pH and planetary climate. *Nature* 560, 471–475.

Keller, C.B., Harrison, T.M. (2020) Constraining crustal silica on ancient Earth. *Proceedings of the National Academy of Sciences* 117, 21101–21107.

Korenaga, J. (2013) Initiation and Evolution of Plate Tectonics on Earth: Theories and Observations. *Annual Review of Earth and Planetary Sciences* 41, 117–151.

Le Maitre, R.W., Streckeisen, A., Zanettin, B., Le Bas, M.J., Bonin, B., Bateman, P. (2005) *Igneous Rocks: A Classification and Glossary of Terms*. Cambridge University Press, Cambridge.

Lipp, A.G., Shorttle, O., Syvret, F., Roberts, G.G. (2020) Major Element Composition of Sediments in Terms of Weathering and Provenance: Implications for Crustal Recycling. *Geochemistry, Geophysics, Geosystems* 21, e2019GC008758.

McKenzie, N.R., Horton, B.K., Loomis, S.E., Stockli, D.F., Planavsky, N.J., Lee, C.-T.A. (2016) Continental arc volcanism as the principal driver of icehouse-greenhouse variability. *Science* 352, 444–447.

Peters, S.E., Husson, J.M., Czaplewski, J. (2018) Macrostrat: A Platform for Geological Data Integration and Deep-Time Earth Crust Research. *Geochemistry, Geophysics, Geosystems* 19, 1393–1409.

Ptáček, M.P., Dauphas, N., Greber, N.D. (2020) Chemical evolution of the continental crust from a data-driven inversion of terrigenous sediment compositions. *Earth and Planetary Science Letters* 539, 116090.

Raymo, M.E., Ruddiman, W.F. (1992) Tectonic forcing of late Cenozoic climate. *Nature* 359, 117–122.

Reimink, J.R., Chacko, T., Stern, R.A., Heaman. L.M. (2014) Earth's earliest evolved crust generated in an Iceland-like setting. *Nature Geoscience* 7, 529–533.

Rudnick, R.L., Gao, S. (2003) Composition of the Continental Crust. *Treatise on Geochemistry* 3, 659.

Ryb, U., Eiler, J.M. (2018) Oxygen isotope composition of the Phanerozoic ocean and a possible solution to the dolomite problem. *Proceedings of the National Academy of Sciences* 115, 6602–6607.

Sayles, F.L., Mangelsdorf, P.C. (1979) Cation-exchange characteristics of Amazon River suspended sediment and its reaction with seawater. *Geochimica et Cosmochimica Acta* 43, 767–779.

Tang, M., Chen, K., Rudnick, R.L. (2016) Archean upper crust transition from mafic to felsic marks the onset of plate tectonics. *Science* 351, 372–375.

Taylor, S.R., McLennan, S.M. (1986) The chemical composition of the Archaean crust. *Geological Society, London, Special Publications* 24, 173–178.

Veizer, J., Godderis, Y., Francois, L.M. (2000) Evidence for decoupling of atmospheric CO_2 and global climate during the Phanerozoic eon. *Nature* 408, 698–701.

Walker, J.C.G., Hays, P.B., Kasting, J.F. (1981) A negative feedback mechanism for the long-term stabilization of Earth's surface temperature. *Journal of Geophysical Research: Oceans* 86, 9776–9782.